Behavioral/Systems/Cognitive

Serotonin Receptor 5-HT_{2B} Mediates Serotonin-Induced Mechanical Hyperalgesia

Shih-Yuan Lin, Wei-Jen Chang, Chih-Shin Lin, Chun-Ying Huang, Hui-Fang Wang, and Wei-Hsin Sun
Department of Life Sciences, National Central University, Jhongli 32054, Taiwan

Serotonin [5-hydroxytryptamine (5-HT)] released from mast cells or platelets in peripheral tissues is one of the important inflammatory mediators in pain and hyperalgesia. The involvement of 5-HT in pain is complex because it could inhibit or facilitate nociceptive transmission, reflecting the presence of multiple 5-HT subtype receptors on peripheral and central nociceptors. The present study aimed to investigate the involvement of 5-HT_{2B} in 5-HT-induced pain and whether the subtype exists in dorsal root ganglion (DRG) neurons. Injecting the 5-HT or 5-HT_2 agonist in hindpaws of mice induced significant hyperalgesia to mechanical stimuli, which was inhibited by the 5-$HT_{2B/2C}$ antagonist but not by 5-HT_{1A}, 5-HT_{2A}, or 5-HT_{3A} antagonists. Therefore, 5-HT_{2B} or 5-HT_{2C} may be involved in 5-HT-induced mechanical hyperalgesia. The 5-$HT_{2B/2C}$ antagonist also blocked 5-HT-induced transient [Ca^{2+}] signaling in DRG neurons. All subtypes of 5-HT receptors except 5-HT_{2C} and 5-HT_6 are present in DRGs. *In situ* hybridization also demonstrated 5-HT_{2B} mainly expressed in small- to medium-diameter DRG neurons that respond to pain. Likely, 5-HT_{2B} mediates 5-HT-induced mechanical hyperalgesia in mice.

Introduction

Tissue injury, infection, or tumor growth, often accompanied by inflammation, produces various chemical mediators, such as prostaglandin E_2, bradykinin, serotonin [5-hydroxytryptamine (5-HT)], and protons, that sensitize pain-transducing neurons (nociceptors) to elicit pain and hyperalgesia (Dray, 1995; Kress and Reeh, 1996; Reeh and Steen, 1996). 5-HT released from platelets, mast cells, and endothelial cells into the inflamed site is proinflammatory and pronociceptive, exciting nociceptive afferents and inducing hyperalgesia (Kessler et al., 1992; Sufka et al., 1992; Taiwo and Levine, 1992; Ernberg et al., 2000; Schmelz et al., 2003; Sommer, 2004). Seven subgroups of serotonin receptors (5-$HT_{1–7}$) have been identified, and some subtypes have more than one receptor (e.g., 5-HT_1 has 5-HT_{1A}, 5-HT_{1B}, 5-HT_{1D}, 5-HT_{1E}, 5-HT_{1F}, and 5-HT_2 has 5-HT_{2A}, 5-HT_{2B}, and 5-HT_{2C}) (Hoyer et al., 2002). The presence of multiple 5-HT receptors on afferent nociceptors reflects distinct mechanisms of 5-HT-induced pain or hyperalgesia through different receptors.

Ionotropic 5-HT_3 is responsible for inflammatory pain (Eschalier et al., 1989; Giordano and Rogers, 1989; Zeitz et al., 2002; Kayser et al., 2007). Lack of the 5-HT_3 gene in mice or blocking by the 5-HT_3 antagonist granisetron elicits normal acute pain responses but reduced responses to persistent pain (Zeitz et al., 2002; Kayser et al., 2007). Giordano and Dyche (1989) showed that 5-HT_3 contributes to chemical but not thermal and mechanical nociceptive pain. Taiwo and Levine (1992) reported that only the 5-HT_{1A} agonist, but not 5-HT_2 or 5-HT_{3A} agonists, mimics the 5-HT effect to induce hyperalgesia and that 5-HT_{1A} antagonists block mechanical hyperalgesia induced by 5-HT. Nevertheless, Kayser et al. (2007) suggested that mice lacking 5-HT_{1A} exhibit increased sensitivity to heat-evoked nociceptive pain but not mechanical pain. The other study of formalin testing suggested that 5-HT_{1A} mediates antinociception (Granados-Soto et al., 2010). In the study by Tokunaga et al. (1998), only the 5-HT_{2A} agonist, but not 5-HT_{1A} and 5-HT_{3A} agonists, mimics 5-HT-induced thermal hyperalgesia, which is blocked by the 5-HT_{2A} antagonist, ketanserin. 5-HT_{2A} also potentiates the effects of other inflammatory mediators (Abbott et al., 1996, 1997). Sufka et al. (1992) suggested that all of the 5-HT_{1A}, 5-HT_{2A}, and 5-HT_3 subtypes also participate in 5-HT-induced pain. In addition, 5-HT_4 enhances the inflammatory pain signal (Doak and Sawynok, 1997). 5-HT_7 inhibits capsaicin-induced mechanical sensitivity (Brenchat et al., 2009).

Many contrary results of 5-HT-receptor mediation in hyperalgesia remain to be resolved. At present, the role played in nociception by 5-HT_{2B} has not been thoroughly investigated, mainly because the presence of 5-HT_{2B} in DRGs is controversial. A previous study by Wu et al. (2001) found no 5-HT_{2B} or 5-HT_{2C} mRNA present in rat DRGs, but Nicholson et al. (2003) found 5-HT_{2B} but not 5-HT_{2C} present. In the present study, we investigated the involvement of 5-HT_{2B} in 5-HT-induced hyperalgesia and found 5-HT_{2B} present in DRG neurons and that the 5-$HT_{2B/2C}$ antagonist 3,5-dihydro-5-methyl-*N*-3-pyridinylbenzo[1,2-b:4,5-b′]dipyrrole-1(2*H*)-carboxamide hydrochloride (SB206553) inhibited 5-HT-induced mechanical hyperalgesia but not thermal hyperalgesia. SB206553 also inhibited 5-HT-induced transient [Ca^{2+}] signaling in DRG neurons. Given that 5-HT_{2B} but not 5-HT_{2C} was present in nociceptors, the 5-HT_{2B} receptor is the one most likely involved in 5-HT-induced mechanical hyperalgesia.

Received Sept. 5, 2010; revised Nov. 12, 2010; accepted Nov. 16, 2010.

This work was supported by National Science Council (Taiwan) Grants NSC 95-2311-B-008-004 and NSC 99-2320-B-008-001-MY3. We thank the support of the Biophysics and Soft Matter at National Central University for calcium imaging.

Correspondence should be addressed to Dr. Wei-Hsin Sun, Department of Life Sciences, National Central University, Jhongda Road 300, Jhongli 32054, Taiwan. E-mail: weihsin@cc.ncu.edu.tw.

DOI:10.1523/JNEUROSCI.4682-10.2011

 0270-6474/11/311410-09$15.00/0

Table 1. Oligonucleotide sequences for quantitative PCR

Genes	Accession no.	Forward primers	Reverse primers	Size (bp)
5-HT1A	NM_008308	5′-TCTGTGAGAGCAGTTGCCACAT	5′-AGCGGCAGAACTTGCACTTGAT	189
5-HT1B	NM_010482	5′-TCGTCGGATATCACCTGTTGCACT	5′-TCACAAAGCAGTCCAGCATCTCCT	227
5-HT1D	NM_008309	5′-TTATCACAGGCTCTGCTGGCTCTT	5′-AGGCAACCAGCAGATGATAAAGGC	218
5-HT1F	NM_008310	5′-AGCAGCAAGGACACTGTACCACAA	5′-TCCGTTGATGGATCGGACAAGGAT	153
5-HT2A	NM_172812	5′-TGCCGTCTGGATTTACCTGGATGT	5′-TACGGATATGGCAGTCCACACCAT	169
5-HT2B	NM_008311	5′-AGGAAATGAAGCAGACTGTGGAGG	5′-CAGTGCAACAGCCAGAATCACAAG	122
5-HT2C	NM_008312	5′-ATAGCCGGTTCAATTCGCGGACTA	5′-TGCTTTCGTCCCTCAGTCCAATCA	114
5-HT3	NM_013561	5′-TCTTGCTGCCCAGTATCTTCCTCA	5′-TTATGCACCAGCCGCACAATGAAG	248
5-HT4	NM_008313	5′-AATGCAAGGCTGGAACAACATCGG	5′-TGTATCTGCTGGGCATGCTCCTTA	210
5-HT5A	NM_008314	5′-GTTTGTGCTCTGCTGGTTCCCTTT	5′-AGCACTGCTGTAGCTCCTGTTGAA	166
5-HT6	NM_021358	5′-TCCATTCTCAACCTCTGCCTCA	5′-TGTTCGAGCTTTGCCCAGTT	187
5-HT7	NM_008315	5′-TCTTCGGATGGGCTCAGAATGT	5′-AACTTGTGTTTGGCTGCGCT	172
GAPDH	NM_001001303	5′-GGAGCCAAACGGGTCATCATCTC	5′-GAGGGGCCATCCACAGTCTTCT	232

Materials and Methods

Cloning of 5-HT$_{2B}$ receptor. Mouse 5-HT$_{2B}$ was cloned into pBSII by PCR. The reaction mixture (50 μl) included 0.2 mM dNTP, 1.5 mM $MgCl_2$, 1 U of *Taq* polymerase, 1× PCR buffer (all Invitrogen), and 500 nM each of primers. A specific primer set for each gene was designed by use of the primer design software Primer3 (http://biotools.umassmed.edu/bioapps/primer3_www.cgi). The primer set for 5-HT$_{2B}$ gene (1677 bp) was as follows (5′–3′, forward/reverse): actgactagttcaccttggctgtgagtgtc/tatctcgaggaagctggacagccttggta. The PCR condition was 1 cycle of 5 min at 95°C, 36 cycles of 45 s at 95°C, 1.5 min at 60°C, 3 min at 72°C, and 1 cycle of 3 min at 72°C. The clone was sequenced and the sequences were matched with the accession number (NM_008311) of the NCBI database. The sequenced clone was further subcloned into pIRES-GFP for expression analysis. 5-HT$_{1A}$, 5-HT$_{2A}$, and 5-HT$_{3A}$ clones were from the Guthrie cDNA Resource Center (Sayre, PA).

Animals. Male CD-1/ICR mice (8–18 weeks of age) were bred and cared for in accordance with the *Guide for the Care and Use of Laboratory Animals*. Animal experimental procedures were approved by the local animal use committee (Institutional Animal Care and Use Committee, National Central University, Taiwan).

Animal tissue and RNA preparation. Tissues from 8- to 12-week-old wild-type mice (CD-1/ICR strain) were removed by use of a fine forceps and immediately frozen in dry ice or in freezing solution for RNA preparation or *in situ* hybridization, respectively. Total RNA from tissues was extracted by use of Trizol reagent (Invitrogen) according to the manufacturer's instructions. RNA was then treated with DNaseI (Roche) at 1.4 U/μg RNA at 37°C for 5 min to remove contamination of genomic DNA for cDNA synthesis. DRG and trigeminal ganglion (TRG) RNA extraction involved the RNeasy kit (QIAGEN).

Reverse transcription-PCR and quantitative PCR. One to 5 μg of total RNA from different mouse tissues was reverse transcribed by use of Superscript II RT (Invitrogen), with oligo-dT (Invitrogen) used as a primer. Derived cDNA was used as a template for PCR experiments. The reaction mixture (10 μl) included 0.2 mM dNTP, 1.5 mM $MgCl_2$, 0.5 U of *Taq* polymerase, 1× PCR buffer, and 100 nM each of primers. The primer sets for 5-HT receptor genes and glyceraldehyde-3-phosphate dehydrogenase (GAPDH) gene were designed by use of Primer3 and are listed in Table 1. The PCR conditions were 95°C for 5 min, followed by 40 cycles of 15 s at 95°C, and 1 min at 60°C. PCR product detection was performed in a 4% agarose gel. The internal control was GAPDH measured from the same samples.

For quantitative PCR of 5-HT receptor genes in DRGs, the reaction mixture (25 μl) included 6 μl of 2× master mix (containing SYBR Green I and AmpliTaq Gold DNA polymerase; Applied Biosystems), 100 nM each of primers and cDNA. Each assay was run in quadruplicate for each preparation. The DRG pool had at least 10 ganglia. The cycling conditions were 95°C for 10 min, 40 cycles of 95°C for 15 s, and 60°C for 1 min. PCRs and product detection involved the ABI Prism 7300 detection system. The amplified product was detected by measurement of SYBR Green I, which was added to the initial experiment mixtures. The threshold cycle (Ct) values obtained in experiments indicate the fractional cycle numbers at which the amount of amplified target reached a fixed threshold. The Ct values of both the target and internal reference (GAPDH) were measured from the same samples, and the expression of the target gene relative to that of GAPDH was calculated by the comparative Ct method to obtain the ΔCt. All data are presented as mean ± SEM.

In situ *hybridization and immunohistochemistry. In situ* hybridization was performed as previously described (Huang et al., 2007). Briefly, lumbar 4 DRG tissues were frozen and sectioned in 12-μm-thick slices by use of a cryostat (Leica Microsystems 3510S). After fixation and acetylation, sections were preincubated with hybridization buffer (50% formamide, 4× SSC, 2× Denhardt's solution, and 50 μg/ml tRNA) for 2 h at room temperature. The digoxigenin-UTP (dig) (Roche)-labeled cRNA probes were generated by *in vitro* transcription with T7 and T3 polymerases (Roche) from nucleotide sequences of 5-HT$_{2B}$ (1455~1888; 433 bp; NM_008311) and hybridized to sections overnight at 65°C. Then slides underwent high-stringency washing cycles with SSC buffers, followed by detection with an alkaline phosphatase-conjugated anti-dig antibody (Roche). Development of signals involved use of a mixture of nitroblue tetrazolium chloride (0.45%) and 5-bromo-4-chloro-3′-indolyphosphate *p*-toluidine salt (0.35%) (Sigma-Aldrich). The specificity of hybridization signals was confirmed by a control study of sense cRNA probes.

After detection of hybridization signals, sections were costained with various combinations of primary antibodies, followed by suitable secondary antibodies. All antibodies were diluted in 1× PBS containing 1% BSA. All antibody incubations were performed at 4°C overnight. Primary antibodies were against N52 (1:500; Sigma-Aldrich) or peripherin (PERI) (1:500; Millipore Bioscience Research Reagents). Secondary antibodies were goat anti-mouse IgG conjugated to TRITC (tetramethylrhodamine isothiocyanate) (1:250; Sigma-Aldrich) or goat anti-rabbit IgG conjugated to FITC (1:250; Sigma-Aldrich). Some experiments involved direct staining with IB$_4$-FITC conjugates (12.5 μg/ml; Sigma-Aldrich).

The specimens were examined by use of a 20× objective with a fluorescence microscope (Zeiss; Axiovert 200). The digitized images were captured by MetaMorph software. In general, >1000 neurons from eight sections were counted, and 95% confidence intervals for proportions were estimated. Experiments were repeated three times and one mouse was used for each group each time.

Agents. The following agents were used: 5-HT (Sigma-Aldrich), α-methyl 5-HT (α-m5-HT) (Sigma-Aldrich), 1-methyl-*N*-[(3-endo)-9-methyl-9-azabicyclo[3.3.1]non-3-yl]-1*H*-indazole-3-carboxamide hydrochloride (granisetron hydrochloride) (Tocris Bioscience), 3-[2-[4-(4-fluorobenzoyl)-1-piperidinyl]ethyl]-2,4[1*H*,3*H*]-quinazolinedione tartrate (ketanserin tartrate) (Tocris Bioscience), SB206553 hydrochloride (Tocris Bioscience), (*S*)-*N*-tert-butyl-3-(4-(2-methoxyphenyl)-piperazin-1-yl)-2-phenylpropanamide dihydrochloride [(*S*)-WAY100135 dihydrochloride] (Tocris Bioscience), 1-[6-[[(17b)-3-methoxyestra-1,3,5(10)-trien-17-yl]amino]hexyl]-1*H*-pyrrole-2,5-dione (phospholipase C inhibitor) (U73122) (Sigma-Aldrich), 1-[6-[((17β)-3-methoxyestra-1,3,5[10]-trien-17-yl)amino]hexyl]-2,5-pyrrolidinedione (U73343) (U73122 analog) (Sigma-Aldrich), and pertussis toxin (PTX) (Sigma-Aldrich). For animal experiments, all compounds were diluted into saline before injection. For cell experiments, all compounds were diluted in the HEPES/MES buffer.

Behavioral tests. Right hindpaws of male CD-1/ICR mice (8–18 weeks of age) were injected with 25 μl of agonists, antagonists, or saline using 30 gauge by 1/2 inch needle (BD Biosciences), and then animal behavioral tests were performed. To assess mechanical nociceptive response, animals were tested for withdrawal thresholds to mechanical stimuli (von Frey filaments; Touch-Test; North Coast Medical) applied to the plantar aspect of the hindpaw. Mice ($n = 6\sim8$ per group) were placed on a wire mesh platform in transparent Plexiglas chambers (10 × 8 × 10 cm/chamber), allowed to habituate for 2 h each day, and trained for 2 d before the test. At certain times after mice were injected with agonists or antagonists, we applied a series of von Frey fibers (0.6, 1.0, 1.4, 2.0, 4 g) in ascending order beginning with the finest fiber through the wire mesh onto the plantar surface of both hindpaws of mice. A withdrawal response was considered valid only if the hindpaw was removed completely from the platform. If the paw withdrawal response was ambiguous, the application of fibers was repeated. For each paw, a von Frey fiber was applied five times at 5 s intervals. The paw withdrawal threshold (PWT) was when paw withdrawal was observed in more than three of five applications.

Animals were also tested for thermal nociceptive response to radiant heat applied to the plantar surface of the paw (Hargreaves et al., 1988). Mice ($n = 6\sim8$ per group) were allowed to habituate for at least 2 h in transparent Plexiglas chambers (10 × 8 × 10 cm/chamber) on a glass floor before testing. At certain times after mice were injected with agonists or antagonists, we stimulated the plantar surface of mouse hindpaws with a light bulb (40% intensity, 305 mW/cm^2). The latency to withdrawal of the paw from radiant heat was measured. Measurements from three trials at 1 min intervals in each paw were averaged. We obtained mean basal withdrawal latencies of ~15~17 s in uninjected mice.

Cell culture and transfection. HEK293T cells were seeded on 24 mm poly-D-lysine-coated coverslips and grown in DMEM (Invitrogen) containing 10% fetal bovine serum (FBS). Cells were then transfected with 5-HT$_{1A}$, 5-HT$_{2A}$, 5-HT$_{2B}$, 5-HT$_{3A}$, or pIRES-GFP vector only. Intracellular Ca^{2+} imaging was performed at 19~48 h after transfection.

One day primary DRG cultures were cultured as previously described (Chen et al., 2009). Briefly, mice were preinjected with or without SB206553, and then injected with 5-HT. After 30 min, mouse lumbar 4–6 DRGs were collected in prewarmed serum-free DMEM. DRGs were first treated with 0.125% collagenase IA (Sigma-Aldrich) at 37°C for 1.5 h, and then with 0.25% trypsin (Invitrogen) at 37°C for 15 min. After trypsin digestion, cells were washed once with DMEM containing 10% FBS, and then once with serum-free medium. DRGs were resuspended in 2 ml of serum-free DMEM and then dissociated into single cells by mechanical titration eight times through flame-polished Pasteur pipettes of decreasing tip diameter. Cell suspension was slowly dropped into 10 ml of serum-free DMEM. After 3~5 min, the cell suspension on the top (~10 ml) was collected and centrifuged at 1224 × *g* for 5 min. The cell pellet was suspended and mixed in 400 μl of DMEM containing 10% FBS and seeded on 100 μg/ml poly-L-lysine-coated 24 mm coverslips. After incubation at 37°C for 2 h, cells were supplemented with 1.5 ml of DMEM containing 10% FBS and maintained at 37°C for 16 h before intracellular Ca^{2+} imaging.

Intracellular calcium imaging. Intracellular calcium imaging was performed as previously described (Chen et al., 2009). Briefly, transfected cells grown on coverslips were preincubated at 37°C with 2.5 μM fura-2 acetoxymethyl ester (fura-2 AM) (Invitrogen) for 40 min in HEPES/MES buffer (125 mM NaCl, 1 mM KCl, 5 mM

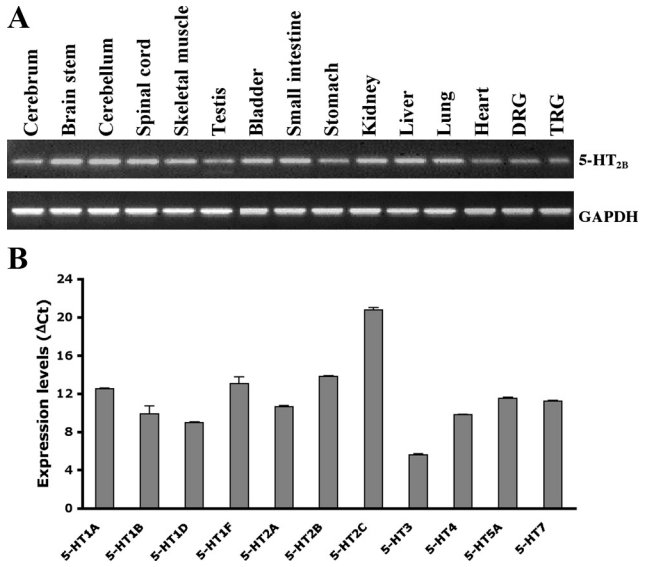

Figure 1. Expression of 5-HT receptor genes. ***A***, Agarose gels showing expression pattern of 5-HT$_{2B}$ in wild-type mouse. RT-PCR results of gene expression of mouse 5-HT$_{2B}$ in different tissues from wild-type mice. Lanes from left to right are cerebrum, brainstem, cerebellum, spinal cord, muscle, testis, bladder, intestine, stomach, kidney, liver, lung, heart, DRG, and TRG, respectively. Mouse GAPDH was an internal control. ***B***, Expression levels of 5-HT receptor subtype genes in DRGs. Quantitative PCR results of relative expression of 5-HT receptor genes were measured. Mouse GAPDH was used as an internal control. Data are presented as mean ± SEM of quadruplicate of the DRG pool. 5-HT$_6$ gene was undetectable and not shown in the figure.

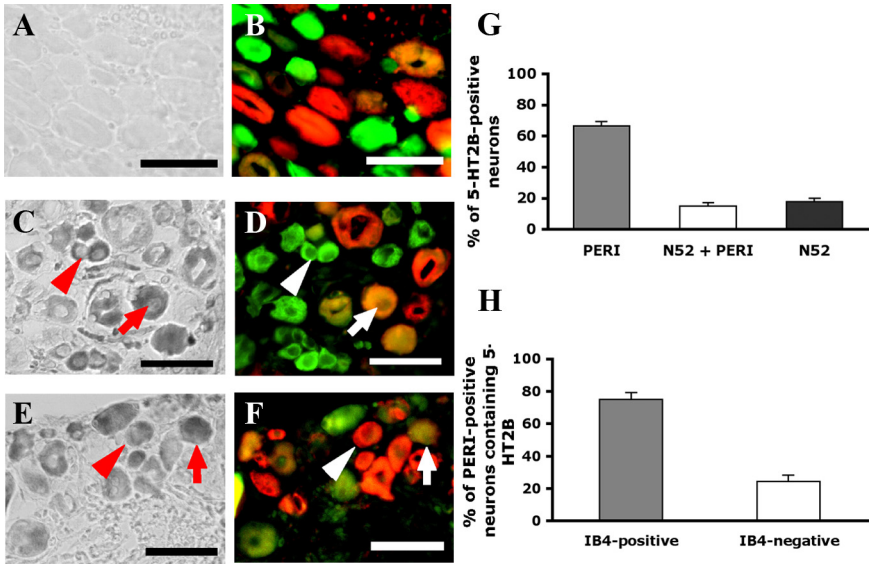

Figure 2. Localization of 5-HT$_{2B}$ receptor in DRG neurons. DRG tissues were sectioned and hybridized with dig-labeled 5-HT$_{2B}$ sense (***A***, ***B***) or antisense cRNA probes (***C–F***), followed by costaining with antibodies. ***A–D***, DRG neurons labeled with 5-HT$_{2B}$ were costained with anti-PERI and anti-N52 antibodies. Phase-contrast fields (***A***, ***C***) are neurons labeled with cRNA probes. Fluorescence images (***B***, ***D***) show neurons labeled with green (PERI only), red (N52 only), and yellow (PERI and N52). The arrowheads indicate the PERI-positive neurons labeled with antisense probes. The arrows are the N52/PERI-positive neurons labeled with antisense probes. Scale bar, 50 μm. ***E***, ***F***, DRG neurons labeled with 5-HT$_{2B}$ were costained with anti-PERI antibodies and IB$_4$-FITC conjugates. Phase-contrast fields (***E***) are neurons labeled with cRNA probes. Fluorescence images (***F***) show neurons labeled with green (IB$_4$ only), red (PERI only), and yellow (PERI and IB$_4$). The arrowheads indicate the PERI-positive neurons labeled with antisense probes. The arrows are the IB$_4$/PERI-positive neurons labeled with antisense probes. Scale bar, 50 μm. ***G***, Histogram showing the proportion of total 5-HT$_{2B}$-positive neurons in PERI, N52, or overlapping subpopulations. A total of 1371 neurons was counted. ***H***, Histogram showing the proportion of total 5-HT$_{2B}$- and PERI-positive neurons in IB$_4$-positive or -negative subpopulations. A total of 1816 PERI-positive neurons was counted. Error bars indicate SEM.

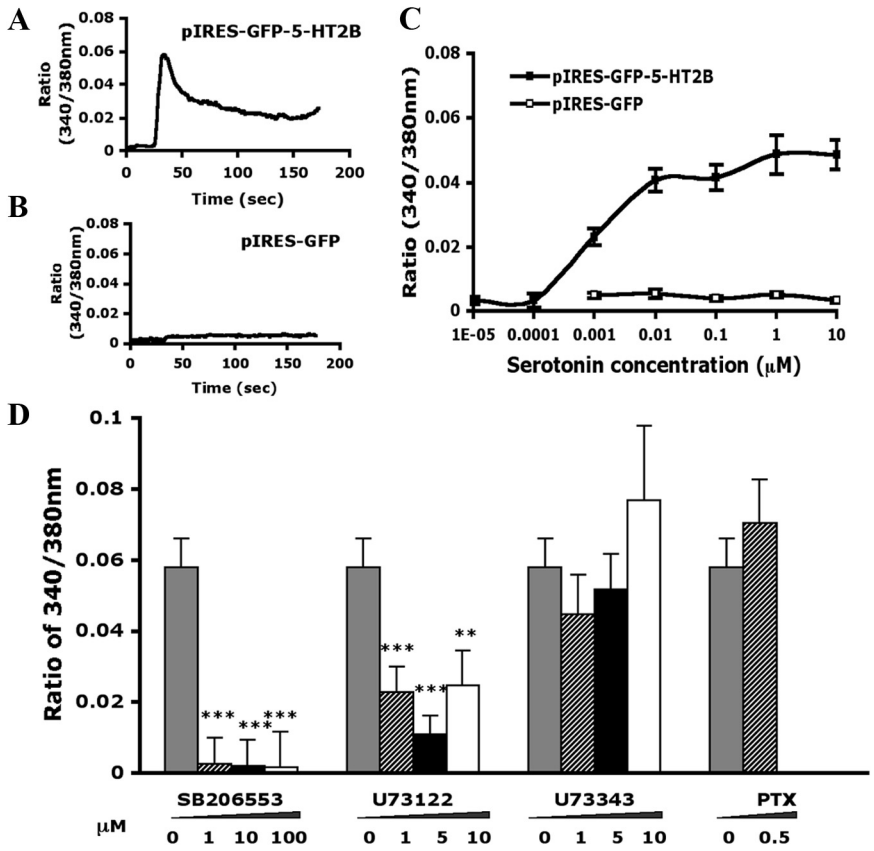

Figure 3. 5-HT$_{2B}$ mediates 5-HT-induced $[Ca^{2+}]_i$ increase in HEK293T cells through the Gq pathway. HEK293T cells were transfected with p-IRES-GFP-5-HT$_{2B}$ or pIRES-GFP. After 48 h, cells were stimulated with different concentrations of 5-HT or with 0.5 μM 5-HT in the presence of different inhibitors (SB206553, U73122, U73343, and PTX), followed by calcium imaging. ***A***, ***B***, Time courses of intracellular calcium signals after the addition of 0.5 μM 5-HT in 5-HT$_{2B}$-expressing cells (***A***) or in vector-expressing cells (***B***) at 25 s. The data represent mean values of 10–15 cells. ***C***, The concentration response curve at 5-HT$_{2B}$ receptors. Data points represent the maximum signal (peak values) obtained at each concentration and are mean ± SEM of at least three independent experiments. Each experiment includes 10~20 cells. ***D***, Histogram showing inhibitor concentration response. Data are mean ± SEM (peak values) of three independent experiments. Comparison between 5-HT- and inhibitor-treated groups (*) was by paired *t* test: $^{**}p < 0.01$; $^{***}p < 0.001$.

$CaCl_2$, 1 mM $MgCl_2$, 8 mM glucose, 10 mM HEPES, and 15 mM MES, pH 7.4). Coverslips were assembled into culture wells and supplemented with 500 μl of the HEPES/MES buffer. Cells were stimulated with 500 μl of HEPES/MES buffer containing twofold concentrations of agonists or antagonists, followed by intracellular calcium recording with a Zeiss inverted microscope equipped with a xenon lamp. Cell images were taken with use of a Zeiss Plan-Apo 63× oil-immersion objective lens. Green fluorescent protein (GFP)-positive cells within a field were identified by use of a FITC filter with excitation wavelength of 480 nm and emission wavelength of 535 nm. In the same field, fura-2 AM fluorescence was measured by 10 Hz alternating wavelength time scanning, with excitation wavelength of 340 and 380 nm and emission wavelength of 510 nm. The fluorescence ratio at two excitation wavelengths (340/380 nm, Ca^{2+}-bound fura-2 AM/free fura-2 AM) was recorded and analyzed.

Statistical analysis. All data are presented as mean ± SEM. Paired Student's *t* test was used for comparison. A value of $p < 0.05$ was considered statistically significant.

Results

5-HT$_{2B}$ is present in nociceptors

A previous study by Wu et al. (2001) suggested that 5-HT$_{2B}$ and 5-HT$_{2C}$ mRNA were not present in rat DRGs, but Nicholson et al. (2003) reported that 5-HT$_{2B}$ but not 5-HT$_{2C}$ was present in rat DRGs. To understand whether 5-HT$_{2B}$ is present in nociceptors, we first examined the tissue distribution of 5-HT$_{2B}$. As shown in Figure 1*A*, 5-HT$_{2B}$ was expressed in all tissues tested. The expression of 5-HT receptor subtypes in DRGs was also examined. Total RNA from DRGs was extracted and 5-HT receptor distribution was analyzed by quantitative PCR. Among subtypes of 5-HT receptors tested (Fig. 1*B*), 5-HT$_6$ was undetectable and 5-HT$_{2C}$ had only a trace amount ($\Delta Ct = 20.75 \pm 0.29$). The highest expressed receptor was 5-HT$_{3A}$ ($\Delta Ct = 5.59 \pm 0.04$). Receptors with the medium levels were 5-HT$_{1B}$, 5-HT$_{1D}$, 5-HT$_{2A}$, and 5-HT$_4$, whereas 5-HT$_{1A}$, 5-HT$_{1F}$, 5-HT$_{2B}$, 5-HT$_5$, and 5-HT$_7$ had lower expression levels (Fig. 1*B*). Localization of 5-HT$_{2B}$ in nociceptors was further examined by *in situ* hybridization. Of the total lumbar 4 DRG neurons, 41% expressed 5-HT$_{2B}$ (Fig. 2). In those 5-HT$_{2B}$-expressed neurons, ~82% were present in PERI-labeled neurons (a marker of small- and medium-diameter neurons) (Fig. 2*C*,*D*,*G*). Of 5-HT$_{2B}$ and PERI-positive populations, 75% were IB$_4$-positive (Fig. 2*E*,*F*,*H*). Accordingly, 5-HT$_{2B}$ was predominantly expressed in nonpeptidergic nociceptors.

The antagonist of 5-HT$_{2B/2C}$, SB206553, inhibits 5-HT$_{2B}$-mediated 5-HT and α-methyl 5-HT signaling *in vitro*

To understand whether the antagonist of 5-HT$_{2B/2C}$, SB206553, inhibits 5-HT$_{2B}$-mediated signaling, we first examined 5-HT$_{2B}$-mediated 5-HT signaling *in vitro*. HEK293T cells overexpressing 5-HT$_{2B}$ were stimulated with different concentrations of 5-HT, and intracellular calcium was measured with a calcium imaging technique. After the addition of 5-HT to the cells, 5-HT$_{2B}$-expressing but not vector-expressing cells showed a rapid increase in intracellular calcium level (Fig. 3*A*,*B*). Effective concentrations of 5-HT caused an increase in calcium level that peaked ~15 s after drug addition. Intracellular calcium levels reached the EC_{50} with 0.001 μM and peaked at 0.01 μM 5-HT (Fig. 3*C*). SB206553 (5-HT$_{2B/2C}$ antagonist) at 1 μM eliminated the increase in 5-HT-induced calcium level in 5-HT$_{2B}$-expressing cells (Fig. 3*D*), thus confirming that 5-HT-induced calcium level increase is mediated by 5-HT$_{2B}$. 5-HT$_{2B}$-expressing cells were treated with U73122 (a phospholipase C inhibitor), which caused a marked inhibition of the 5-HT-induced $[Ca^{2+}]$ increase in level. U73343 (an inactive analog of U73122) or PTX (Gi protein inhibitor) was ineffective in inhibiting the Ca^{2+} response (Fig. 3*D*), which suggests that 5-HT$_{2B}$-mediated signaling is mainly through activation of Gq protein.

To understand whether SB206553 acts only on 5-HT$_{2B}$ and 5-HT$_{2C}$, SB206553 was tested in 5-HT$_{1A}$-, 5-HT$_{2A}$-, 5-HT$_{2B}$-, 5-HT$_{2C}$-, or 5-HT$_{3A}$-expressing cells. As shown in Figure 4*A*, SB206553 (1 μM) inhibited 5-HT$_{2B}$- or 5-HT$_{2C}$-mediated 5-HT signaling but not 5-HT$_{1A}$-, 5-HT$_{2A}$-, or 5-HT$_{3A}$-mediated 5-HT signaling. We also examined whether signaling induced by the selective 5-HT$_2$ agonist α-m5-HT could be inhibited by SB206553. Indeed, α-m5-HT specifically activated 5-HT$_{2A}$, 5-HT$_{2B}$, and 5-HT$_{2C}$, but not 5-HT$_{1A}$ or 5-HT$_3$ (Fig. 4*B*). Interestingly, 1 μM SB206553 com-

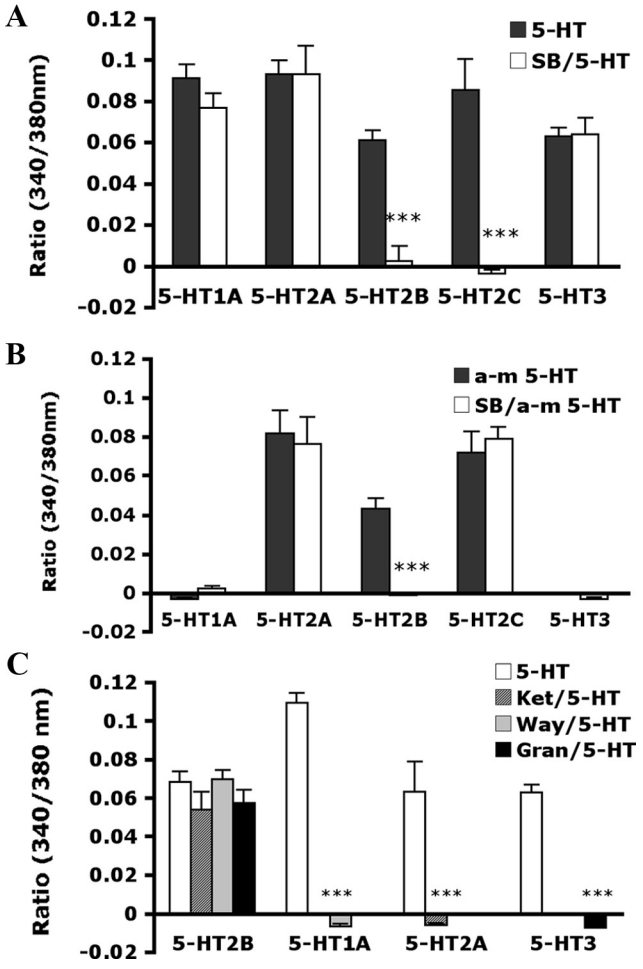

Figure 4. 5-HT- and α-methyl 5-HT-induced $[Ca^{2+}]_i$ increase in HEK293T cells expressing 5-HT receptors. HEK293T cells were transfected with p-IRES-GFP-5-HT$_{2B}$, pcDNA3.1–5-HT$_{1A}$, pcDNA3.1–5-HT$_{2A}$, pcDNA3.1–5-HT$_{2C}$, or pcDNA3.1–5-HT$_{3A}$. After 19 h, cells were stimulated with selective agonists or antagonists, followed by $[Ca^{2+}]_i$ recording. ***A***, The histogram showing the maximum signal obtained from transfected cells after stimulated with 0.5 μM 5-HT in the absence or presence of 1 μM SB206553 (SB). ***B***, Histogram showing the maximum signal obtained from transfected cells after stimulation with 0.5 μM α-methyl 5-HT (α-m5-HT) in the absence or the presence of 1 μM SB. ***C***, Histogram showing the maximum signal obtained from transfected cells after stimulation with 0.5 μM 5-HT in the absence or presence of 1 μM ketanserin (Ket), 10 μM WAY100135 (Way), or 1 μM granisetron (Gran). The data are mean ± SEM of at least three independent experiments. Each experiment contains at least 10∼20 cells. Comparison between agonist- and antagonist-treated groups (*) was by paired *t* test: ***$p < 0.001$.

pletely inhibited α-m5-HT-induced $[Ca^{2+}]$ signaling in 5-HT$_{2B}$-expressing cells (Fig. 4*B*). However, α-m5-HT-induced $[Ca^{2+}]$ signaling in 5-HT$_{2C}$-expressing cells could not be inhibited by 1 μM SB206553. A high concentration (10 μM) of SB206553 was required (data not shown). Selective antagonists for 5-HT$_{1A}$ (WAY100135), 5-HT$_{2A}$ (ketanserin), or 5-HT$_{3A}$ (granisetron) were also tested for specificity. Selective antagonists blocked the mediated signaling of each subtype, but 5-HT$_{2B}$-mediated signaling was not inhibited by any antagonists for 5-HT$_{1A}$, 5-HT$_{2A}$, or 5-HT$_{3A}$ (Fig. 4*C*).

The antagonist of 5-HT$_{2B/2C}$, SB206553, inhibits 5-HT-induced mechanical hyperalgesia but not thermal hyperalgesia

Local administration of 5-HT (10 μM) into mice hindpaws caused pain-related behaviors. Before injection (0 min), the PWT for mechanical stimuli was 3.50 ± 0.42 g on the injected paw

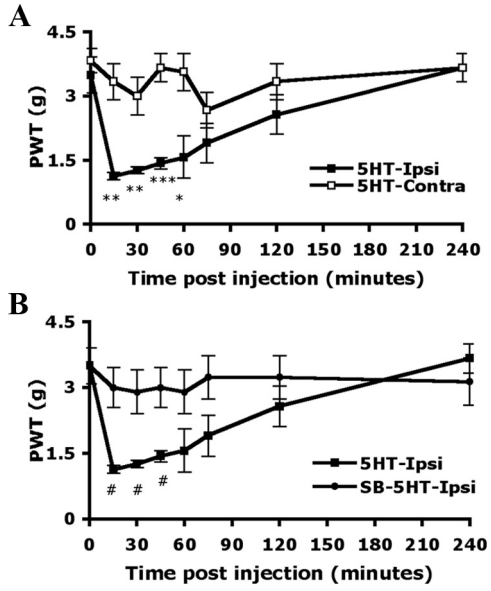

Figure 5. 5-HT-induced mechanical hyperalgesia is inhibited by peripheral injection with the antagonist of 5-HT$_{2B/2C}$. Wild-type CD1/ICR mice (15–18 weeks of age) were preinjected without (***A***) or with (***B***) 25 μl of SB206553 (10 μM), and then with 25 μl of 5-HT (10 μM in saline). The PWT was measured before injection ($t = 0$) and after injection. All data are mean ± SEM of total tested mice ($n = 6$ per group). Comparison between contralateral and ipsilateral sides of 5-HT-injected animals (*) or between 5-HT-injected and SB-5HT-injected animals (#) was by paired *t* test: *#$p < 0.05$; **$p < 0.01$; ***$p < 0.001$.

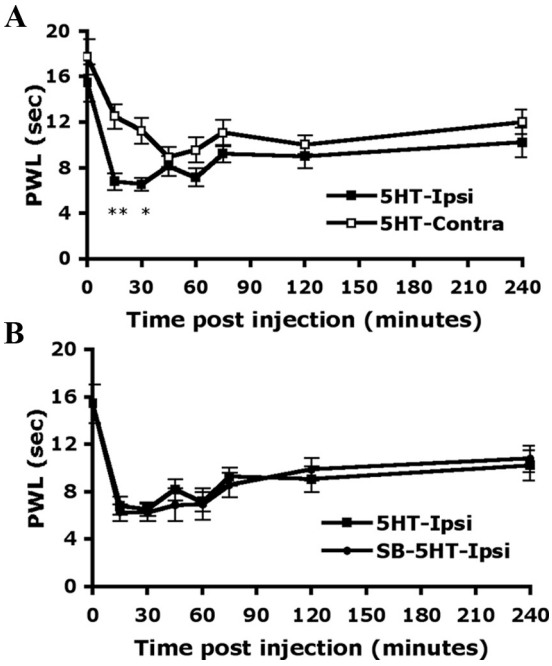

Figure 6. 5-HT-induced thermal hyperalgesia is not inhibited by peripheral injection with the antagonist of 5-HT$_{2B/2C}$. Wild-type CD1/ICR mice (14–18 weeks of age) were preinjected without (***A***) or with (***B***) 25 μl of SB206553 (10 μM), and then with 25 μl of 5-HT (10 μM in saline). The PWL was measured before injection ($t = 0$) and after injection. All data are mean ± SEM of total tested mice ($n = 7$ per group). Comparison between contralateral and ipsilateral sides of 5-HT-injected animals (*) was by paired *t* test: *$p < 0.05$; **$p < 0.01$.

(ipsilateral side) and 3.83 ± 0.29 g on the uninjected paw (contralateral side). The greatest magnitude of pain-related behaviors occurred within 15 min after the injection (PWT = 1.13 ± 0.08 g on the ipsilateral paw and 3.33 ± 0.42 g on the contralateral paw)

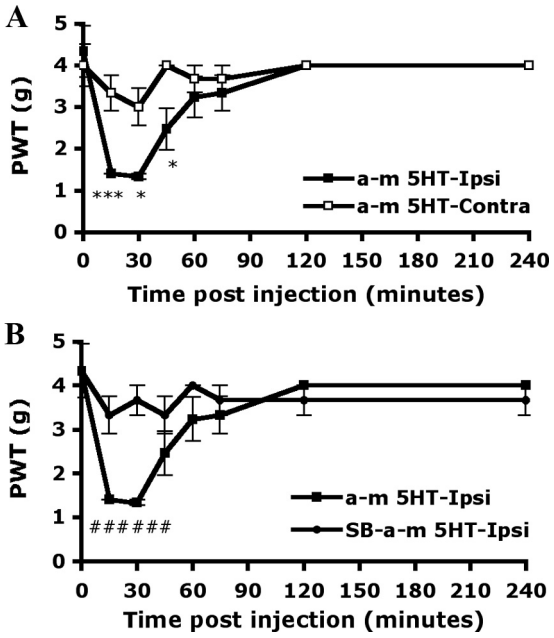

Figure 7. 5-HT$_2$ agonist-induced mechanical hyperalgesia is inhibited by peripheral injection with the antagonist of 5-HT$_{2B/2C}$. Wild-type CD1/ICR mice (8–10 weeks of age) were preinjected without (***A***) or with (***B***) 25 μl of SB206553 (10 μM), and then with 25 μl of α-m5-HT (5 μM in saline). The PWT was measured before injection ($t = 0$) and after injection. All data are mean ± SEM of total tested mice ($n = 6$ per group). Comparison between contralateral and ipsilateral sides of α-m5-HT-injected animals (*) or α-m5-HT-injected and SB-α-m5-HT-injected animals (#) was by paired t test: $^{*}p < 0.05$; $^{***\,\#\#\#}p < 0.001$.

(Fig. 5*A*). The hyperalgesia induced by mechanical stimuli was gradually decreased and returned to baseline within 4 h. Nonnoxious mechanical stimulation did not induce hyperalgesia in saline-injected mice (data not shown). When mice were preinjected with SB206553 (10 μM), an antagonist of 5-HT$_{2B/2C}$, before 5-HT injection, the hyperalgesia to mechanical stimuli was completely inhibited within 15 min after injection (3.00 ± 0.44 g on the ipsilateral paw and 3.67 ± 0.33 g on contralateral paw) (Fig. 5*B*) and the inhibition lasted at least 4 h.

The paw withdrawal latency (PWL) to heat stimuli was also examined on 5-HT-injected mice. The latency of paw withdrawal was 17.75 ± 1.55 s for the contralateral paw and 15.45 ± 1.64 s for the ipsilateral paw before injection. At 15 min after 5-HT injection, the latency was decreased to 6.80 ± 0.73 s for the ipsilateral paw and remained at 12.51 ± 1.07 s for the contralateral paw (Fig. 6*A*). The decreased PWL to heat stimulation gradually returned to baseline after 4 h (10.20 ± 1.30 s on the ipsilateral paw and 12.04 ± 1.09 s on the contralateral paw). Unlike with mechanical hyperalgesia, with thermal hyperalgesia, SB206553 preinjection before 5-HT injection did not block the hyperalgesia (6.27 ± 0.72 s on the ipsilateral paw and 10.04 ± 1.98 s on contralateral paw in 15 min) (Fig. 6*B*).

The antagonist of 5-HT$_{2B/2C}$, SB206553, inhibits 5-HT$_2$ agonist-induced mechanical hyperalgesia

As shown in Figure 5, 5-HT-induced mechanical hyperalgesia was inhibited by the antagonist of 5-HT$_{2B/2C}$. To further confirm that the effect is attributable to 5-HT$_{2B/2C}$ function, we used the 5-HT$_2$ agonist α-m5-HT to induce mechanical hyperalgesia. After being injected with α-m5-HT (5 μM), mice showed hyperalgsia to mechanical stimuli within 15 min. The PWT was 1.40 ± 0.00 and 3.33 ± 0.42 g for the ipsilateral and contralateral paws, respectively (Fig. 7*A*). Hyperalgesia induced by α-m5-HT disappeared within 90 min. The response was shorter than that induced by 5-HT. Preinjection with SB206553 (10 μM) before α-m5-HT injection completely inhibited the mechanical hyperalgesia within 15 min (PWT = 3.33 ± 0.42 and 3.67 ± 0.33 g for the ipsilateral and contralateral paws, respectively) (Fig. 7*B*), and the inhibition lasted until α-m5-HT-induced hyperalgesia disappeared.

The antagonist of 5-HT$_{2A}$, ketanserin, does not inhibit 5-HT or α-m5-HT-induced mechanical hyperalgesia

To understand whether 5-HT$_{2A}$ is involved in 5-HT-induced mechanical hyperalgesia, the selective antagonist of 5-HT$_{2A}$, ketanserin, was used to inhibit 5-HT$_{2A}$ function. When mice were preinjected with ketanserin (10 μM) before 5-HT injection, the hyperalgesia to mechanical stimuli was not inhibited but was slightly enhanced in the first 30 min after injection (PWT = 0.73 ± 0.08 g on the ipsilateral paw of ket-5HT-injected mice and 1.13 ± 0.08 g on ipsilateral paw of 5-HT-injected mice) (Fig. 8*A*). Nevertheless, the hyperalgesia in ket-5HT-injected mice returned to baseline within 60–90

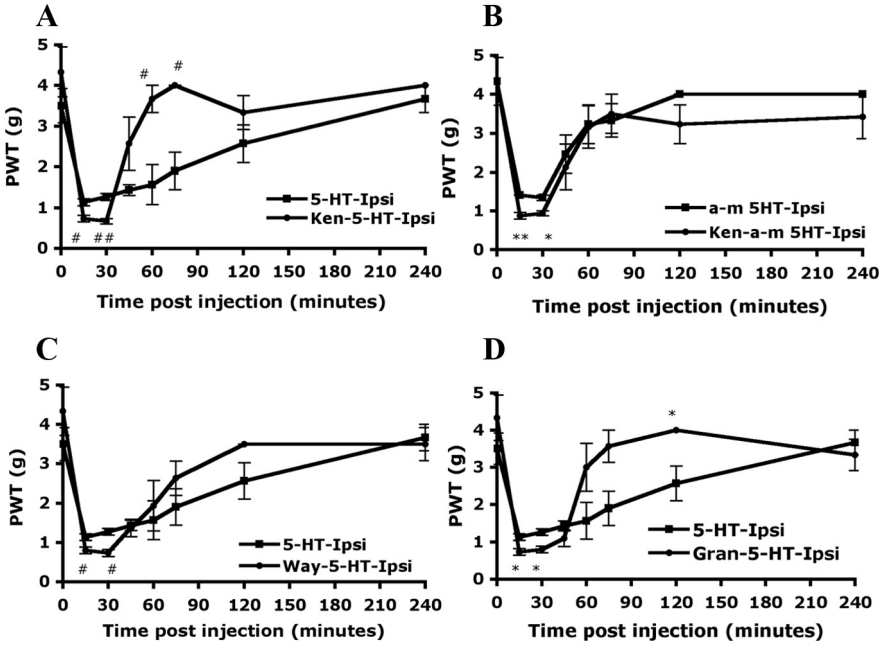

Figure 8. 5-HT-induced mechanical hyperalgesia is not inhibited by peripheral injection with the antagonists of 5-HT$_{1A}$, 5-HT$_{2A}$, or 5-HT$_{3A}$. Wild-type CD1/ICR mice (8–18 weeks of age) were preinjected with or without 25 μl of ketanserin (Ket) (10 μM in saline) (***A***), WAY100135 (Way) (10 μM in saline) (***C***), or granisetron (Gran) (1 μM in saline) (***D***), followed by injection with 25 μl of 5-HT (10 μM in saline) (***A***, ***C***, ***E***) or α-m5-HT (5 μM in saline) (***B***). The PWT was measured before injection ($t = 0$) and after injection. All data are mean ± SEM of total tested mice ($n = 6$ per group). Comparison between 5-HT-injected and ket-5-HT-injected animals (#), between α-m5-HT-injected and ket-α-m5-HT-injected animals (*), between 5-HT-injected and Way-5-HT-injected animals (#), or between 5-HT-injected and Gran-5-HT-injected animals (*) was by paired t test: $^{*\,\#}p < 0.05$; $^{**\,\#\#}p < 0.01$.

min, faster than in 5-HT-injected mice (within 4 h). Similar results were obtained with α-m5-HT injection instead of 5-HT. Ket-α-m5-HT-injected mice, like ket-5-HT-injected mice, also displayed slightly enhanced mechanical hyperalgesia within first 30 min, and hyperalgesia disappeared in 60–90 min (Fig. 8*B*).

Selective antagonists for 5-HT$_{1A}$ or 5-HT$_{3A}$ do not inhibit 5-HT-induced mechanical hyperalgesia

Sufka et al. (1992) found that all 5-HT$_1$, 5-HT$_2$, 5-HT$_3$ subtype receptors were involved in 5-HT-induced pain. Taiwo and Levine (1992) reported that 5-HT$_{1A}$ antagonists blocked mechanical hyperalgesia induced by 5-HT. To understand whether 5-HT$_1$ and 5-HT$_3$ are involved in 5-HT-induced mechanical hyperalgesia, we tested selective antagonists for 5-HT$_1$ or 5-HT$_3$. As shown in Figure 8*C*, the 5-HT$_1$ antagonist WAY100135 did not inhibit but, rather, slightly enhanced 5-HT-induced mechanical hyperalgesia in the first 30 min after injection, and hyperalgesia gradually disappeared in 90–120 min. Similarly, the 5-HT$_3$ antagonist granistetron enhanced 5-HT-induced mechanical hyperalgesia in the first 30 min, but hyperalgesia disappeared in 60–90 min (Fig. 8*D*).

The antagonist of 5-HT$_{2B/2C}$, SB206553, inhibited 5-HT-induced signaling in DRG neurons

To examine the effect of SB206553 on DRG neurons, we collected lumbar 4–6 DRG neurons from 5-HT-injected and SB-5-HT-injected mice at 30 min after injection and analyzed 5-HT-induced signaling. In DRGs from the contralateral side of 5-HT-injected mice, 3.4% of DRG neurons responded to 1 μM 5-HT stimuli and elicited an increase in [Ca^{2+}] level with two different patterns (Fig. 9*A*,*B*) in 10- to 35-μm-diameter neurons. Pattern 1 was a rapid [Ca^{2+}] level increase after 5-HT stimulation; and pattern 2 was a rapid [Ca^{2+}] level increase followed by a sustained and delayed return. The number of 5-HT-responding neurons in DRGs from the ipsilateral side of 5-HT-injected mice was twofold higher than those from the contralateral side (8.5 vs 3.4%). Only pattern 1 showed an increased [Ca^{2+}] response (increased peak value 4.5-fold) (Fig. 9*C*,*E*). The peak value of pattern 2 did not change (Fig. 9*D*). In contrast, DRG neurons from SB-5-HT-injected mice showed few responding cells (2.9% 5-HT responding neurons on the ipsilateral side). Patterns 1 disappeared on the ipsilateral side of SB206553 injection but was unchanged on the contralateral side (Fig. 9*E*). A transient [Ca^{2+}] response in pattern 2 also disappeared on the ipsilateral side, but sustained [Ca^{2+}] response remained. It seems that transient [Ca^{2+}] response is completely eliminated after SB206553 injection. Accordingly, the results provide the evidence that 5-HT injection increased 5-HT receptors for the 5-HT response in peripheral neurons, and SB206553 inhibited peripheral 5-HT$_{2B/2C}$ action, thus reducing the 5-HT response.

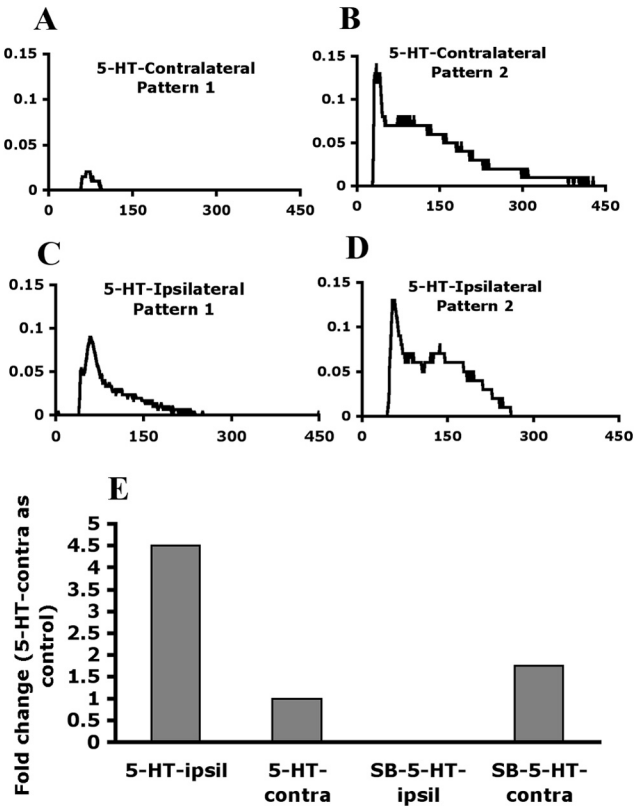

Figure 9. 5-HT-induced [Ca^{2+}]$_i$ increase in primary DRG neurons is inhibited by SB206553. Primary DRGs were taken from 5-HT-injected or SB-5-HT-injected mice at 30 min after injection and cultured for 12~16 h. Cultured neurons were stimulated with 1 μM 5-HT, followed by calcium imaging. Shown are time courses of intracellular calcium signals after addition of 1 μM 5-HT in 5-HT-injected contralateral DRG neurons (***A***, ***B***) and ipsilateral DRG neurons (***C***, ***D***). ***E***, Histograms showing fold change of peak value in pattern 1. In 5-HT-injected group, six independent experiments were done, and three mice were used in each experiment (total 18 mice). Totals of 88 neurons and 94 neurons were counted in the contralateral side and in the ipsilateral side, respectively. In SB-5-HT-injected group, seven independent experiments were done, and three or four mice were used in each experiment (total 26 mice). Totals of 79 neurons and 88 neurons were counted in the contralateral side and in the ipsilateral side, respectively.

Discussion

In this study, we investigated the involvement of 5-HT$_{2B}$ in 5-HT-induced pain. The selective antagonist for 5-HT$_{2B/2C}$, SB206553, but not antagonists for 5-HT$_{1A}$, 5-HT$_{2A}$, or 5-HT$_{3A}$, completely inhibited 5-HT-induced mechanical hyperalgesia. SB206553 injection in mice also inhibited DRG neurons responding to 5-HT. Given that only a trace amount of 5-HT$_{2C}$ mRNA is detected in DRG tissues (Fig. 1), 5-HT$_{2B}$ seems to be the subtype mediating 5-HT-induced mechanical hyperalgesia.

The roles of 5-HT$_{2B}$ in 5-HT-induced pain were previously overlooked, mainly because the presence of 5-HT$_{2B}$ in rat DRGs is arguable. Wu et al. (2001), using reverse transcription (RT)-PCR, could not detect 5-HT$_{2B}$ mRNA in DRGs, whereas Nicholson et al. (2003), using *in situ* hybridization, reported 5-HT$_{2B}$ in rat DRGs. To clarify this issue, we used both techniques to examine the presence of 5-HT$_{2B}$ in mouse DRGs and found 5-HT$_{2B}$ mRNA in mouse DRGs, although the expression was at a medium level compared with that of other 5-HT subtype receptors. Consistent with previous results from Nicholson et al. (2003), we also found that 5-HT$_{2B}$ was distributed in small-, medium-, and large-diameter DRG neurons but mainly in the small-to-medium population (82% of total 5-HT$_{2B}$-positive neurons). Nicholson et al. reported almost 100% rat DRG neurons expressing 5-HT$_{2B}$, whereas we found 41% of mouse DRG neurons expressing 5-HT$_{2B}$. Of 5-HT$_{2B}$- and PERI-coexpressing neurons, most (75%) were in IB$_4$-positive neurons. The distribution of 5-HT$_{2B}$ in DRGs suggests its possible involvement in pain.

Sufka et al. (1992) found all 5-HT$_1$, 5-HT$_2$, 5-HT$_3$ subtype receptors involved in 5-HT-induced pain. However, Taiwo and Levine suggested that the 5-HT$_1$ agonist but not 5-HT$_2$ or 5-HT$_3$ agonist induces 5-HT-induced hyperalgesia. Tokunaga et al. (1998) found that rats displayed thermal hyperalgesia on injection with the 5-HT$_2$ agonist but not 5-HT$_1$ or 5-HT$_3$ agonist. In this study, we demonstrated that 5-HT-induced mechanical hyperalgesia can be com-

pletely inhibited by the 5-HT$_{2B/2C}$ antagonist, SB206553, but not by antagonists for 5-HT$_{1A}$, 5-HT$_{2A}$, or 5-HT$_3$.

We found that the 5-HT$_3$ antagonist, granisetron, did not inhibit mechanical hyperalgesia but shortened the hyperalgesia response. 5-HT$_3$ is responsible for direct action in chemical stimuli but not in the mechanical or thermal response (Giordano and Dyche, 1989). Although Zeitz et al. (2002) showed that mice lacking 5-HT$_3$ have a reduced visceral pain response after injection of 5-HT, mice injected with the 5-HT$_3$ agonist did not display mechanical hyperalgesia (Taiwo and Levine, 1992) or thermal hyperalgesia (Tokunaga et al., 1998). Thus, our data are consistent with previous results that 5-HT$_3$ is not involved in 5-HT-induced mechanical hyperalgesia. Our finding that the 5-HT$_3$ antagonist shortened the mechanical hyperalgesia response and other findings that lack of or blocking the 5-HT$_3$ with an antagonist also show reduced responses in the phase 2 of formalin-induced nociception (Kayser et al., 2007) suggest that 5-HT$_3$ may have an influence on maintaining hyperalgesia but does not directly act on mechanical hyperalgesia.

5-HT$_{1A}$ has been found to be involved in 5-HT-induced mechanical hyperalgesia (Taiwo and Levine, 1992). In contrast, our findings suggested that the 5-HT$_{1A}$ antagonist cannot inhibit 5-HT-induced mechanical hyperalgesia but slightly enhanced hyperalgesia in the first 30 min. The difference between our results and those of Taiwo and Levine could be attributable to the antagonists and measurement methods used. Taiwo and Levine used spiperone, which has considerable affinities for 5-HT$_2$ and dopamine (D$_2$) receptors, so the inhibition could be attributable in part to action of these receptors. In our study, we used a more selective antagonist, WAY100135, which acts on 5-HT$_{1A}$ but not 5-HT$_2$ or 5-HT$_3$ in a cultured system. Other studies involving the same antagonist also did not find 5-HT$_{1A}$ involved in mechanical hyperalgesia (Parada et al., 2001; Kayser et al., 2007). The role of 5-HT$_{1A}$ in 5-HT-induced pain seems more complicated. Millan (1994) found that 5-HT$_{1A}$ agonists mediated antinociception under certain conditions. A formalin test study also suggested that 5-HT$_{1A}$ mediates antinociception (Granados-Soto et al., 2010). Mice lacking 5-HT$_{1A}$ exhibit increased sensitivity to heat-evoked nociceptive pain but not mechanical pain (Kayser et al., 2007). In our data, 5-HT$_{1A}$ seems to have few antinociceptive effects on 5-HT-induced mechanical hyperalgesia, because 5-HT$_{1A}$ only slightly enhanced mechanical hyperalgesia.

A previous study by Tokunaga et al. (1998) suggested that the 5-HT$_2$ agonist, α-m5-HT, mimics the 5-HT-induced response. Similarly, we demonstrated that α-m5-HT can induce mechanical hyperalgesia, but hyperalgesia disappeared shortly, within 60–90 min. In cell experiments, α-m5-HT acted on 5-HT$_{2A}$ and on 5-HT$_{2B}$ and 5-HT$_{2C}$, which suggests that α-m5-HT-induced mechanical hyperalgesia may act on 5-HT$_{2A}$, 5-HT$_{2B}$, or 5-HT$_{2C}$. 5-HT$_{2A}$ and 5-HT$_{2B/2C}$ antagonists inhibited the α-m5-HT action in 5-HT$_{2A}$-, 5-HT$_{2B}$-, or 5-HT$_{2C}$-expressing cells, respectively. However, α-m5-HT-induced mechanical hyperalgesia can be inhibited by only the 5-HT$_{2B/2C}$ antagonist, not the 5-HT$_{2A}$ antagonist. Similarly, the 5-HT$_{2A}$ antagonist did not inhibit 5-HT-induced mechanical hyperalgesia.

A previous study suggested that the 5-HT$_{2A}$ antagonist ketanserin inhibits 5-HT-induced thermal hyperalgesia but not mechanical hyperalgesia in rats (Tokunaga et al., 1998). In contrast, the 5-HT$_{2B/2C}$ antagonist, SB206553, inhibited 5-HT-induced mechanical hyperalgesia but not thermal hyperalgesia. 5-HT$_2$ subtype receptors seem to be responsible for 5-HT-induced hyperalgesia: 5-HT$_{2A}$ for thermal hyperalgesia and 5-HT$_{2B}$ or 5-HT$_{2C}$ for mechanical hyperalgesia. Given that 5-HT$_{2C}$ has only trace amounts in DRGs and 5-HT-induced hyperalgesia occurred within 15 min, 5-HT$_{2C}$ is unlikely synthesized in such a short time. In addition, a high concentration of SB206553 was required to block α-m5-HT action on 5-HT$_{2C}$-expressing cells, which suggests that 5-HT$_{2B}$ is more sensitive to SB206553. The study by Knight et al. (2004) had reported that 5-HT$_{2A}$ antagonist, ketanserin, is also a potent blocker of the 5-HT$_{2C}$ receptor. Ketanserin did not inhibit 5-HT-induced mechanical hyperalgesia. Accordingly, 5-HT$_{2B}$ seems to be the subtype involved in 5-HT-induced mechanical hyperalgesia.

In DRG neurons from 5-HT-injected mice, the number of 5-HT-responding neurons was increased in the ipsilateral side (from 3.4 to 8.5%), and the [Ca^{2+}] response only increased in pattern 1. All responding cells were mainly located in 10~35 μm, which is consistent with results from *in situ* hybridization that 5-HT$_{2B}$ was expressed predominantly in small- to medium-diameter neurons. After SB206553 injection, the number of 5-HT-responding cells was decreased to 2.9% on the ipsilateral side. SB206553 inhibited the [Ca^{2+}] response in patterns 1 and partially in pattern 2, which suggests that patterns 1 and the transient [Ca^{2+}] response in pattern 2 are mediated by the 5-HT$_{2B}$ or 5-HT$_{2C}$ receptor. Because 5-HT$_{2C}$ showed only trace amounts in DRG neurons, 5-HT$_{2B}$ could be the only receptor mediating 5-HT-induced transient [Ca^{2+}] signaling. Given that 5-HT$_{2B}$ gene expression in DRGs did not have significant change after 5-HT injection (data not shown), the increased number of 5-HT-responding neurons could not be attributable to an increase in the number of 5-HT$_{2B}$ receptors. More likely, it is because 5-HT$_{2B}$-mediated signaling is enhanced.

How 5-HT$_{2B}$ mediates 5-HT-induced mechanical hyperalgesia is unclear. Several lines of evidence have suggested that 5-HT increased tetrodotoxin-resistant (TTX-R) I_{Na} currents (Gold et al., 1996), Nav1.8 (one of TTX-R channels) is related to inflammatory hyperalgesia (Abrahamsen et al., 2008), and protein kinase C (PKC) can modulate TTX-R I_{Na} currents (Gold et al., 1998; Cang et al., 2009). Given that 5-HT$_{2B}$ activation leads to PKC activation, 5-HT$_{2B}$-mediated mechanical hyperalgesia may be attributable to modulation of TTX-R I_{Na} currents through PKC. A recent study has also found that one isoform of PKC, PKCε, can mediate mechanical hyperalgesia by mitochondrial mechanisms (Joseph and Levine, 2010). Alternatively, 5-HT$_{2B}$ mediates mechanical hyperalgesia by activating a PKCε-dependent mitochondrial mechanism.

References

Abbott FV, Hong Y, Blier P (1996) Activation of 5-HT2A receptors potentiates pain produced by inflammatory mediators. Neuropharmacology 35:99–110.

Abbott FV, Hong Y, Blier P (1997) Persisting sensitization of the behavioural response to formalin-induced injury in the rat through activation of serotonin2A receptors. Neuroscience 77:575–584.

Abrahamsen B, Zhao J, Asante CO, Cendan CM, Marsh S, Martinez-Barbera JP, Nassar MA, Dickenson AH, Wood JN (2008) The cell and molecular basis of mechanical, cold, and inflammatory pain. Science 321:702–705.

Brenchat A, Romero L, García M, Pujol M, Burgueño J, Torrens A, Hamon M, Baeyens JM, Buschmann H, Zamanillo D, Vela JM (2009) 5-HT7 receptor activation inhibits mechanical hypersensitivity secondary to capsaicin sensitization in mice. Pain 141:239–247.

Cang CL, Zhang H, Zhang YQ, Zhao ZQ (2009) PKCε-dependent potentiation of TTX-resistant Na$_v$1.8 current by neurokinin-1 receptor activation in rat dorsal root ganglion neurons. Mol Pain 5:33.

Chen YJ, Huang CW, Lin CS, Chang WH, Sun WH (2009) Expression and function of proton-sensing G protein-coupled receptors in inflammatory pain. Mol Pain 5:39.

Doak GJ, Sawynok J (1997) Formalin-induced nociceptive behavior and

edema: involvement of multiple peripheral 5-hydroxytryptamine receptor subtypes. Neuroscience 80:939–949.

Dray A (1995) Inflammatory mediators of pain. Br J Anaesth 75:125–131.

Ernberg M, Lundeberg T, Kopp S (2000) Effect of propranolol and granisetron on experimentally induced pain and allodynia/hyperalgesia by intramuscular injection of serotonin into the human masseter muscle. Pain 84:339–346.

Eschalier A, Kayser V, Guilbaud G (1989) Influence of a specific 5-HT3 antagonist on carrageenan-induced hyperalgesia in rat. Pain 36:249–255.

Giordano J, Dyche J (1989) Differential analgesic actions of serotonin 5-HT3 receptor antagonists in the mouse. Neuropharmacology 28:423–427.

Giordano J, Rogers LV (1989) Peripherally administered serotonin 5-HT3 rceptor antagonists reduce inflammatory pain in rats. Eur J Pharmacol 170:83–86.

Gold MS, Reichling DB, Shuster MJ, Levine JD (1996) Hyperalgesic agents increase a tetrodotoxin-resistant Na^+ current in nociceptors. Proc Natl Acad Sci U S A 93:1108–1112.

Gold MS, Levine JD, Correa AM (1998) Modulation of TTX-R I_{Na} by PKC and PKA and their role in PGE_2-induced sensitization of rat sensory neurons *in vitro*. J Neurosci 18:10345–10355.

Granados-Soto V, Argüelles CF, Rocha-González HI, Godínez-Chaparro B, Flores-Murrieta FJ, Villalón CM (2010) The role of peripheral 5-HT_{1A}, 5-HT_{1B}, 5-HT_{1D}, 5-HT_{1E} and 5-HT_{1F} serotonergic receptors in the reduction of nociception in rats. Neuroscience 165:561–568.

Hargreaves K, Dubner R, Brown F, Flores C, Joris J (1988) A new and sensitive method for measuring thermal nociception in cutaneous hyperalgesia. Pain 32:77–88.

Hoyer D, Hannon JP, Martin GR (2002) Molecular, pharmacological and functional diversity of 5-HT receptors. Pharmacol Biochem Behav 71:533–554.

Huang CW, Tzeng JN, Chen YJ, Tsai WF, Chen CC, Sun WH (2007) Nociceptors of dorsal root ganglion express proton-sensing G-protein-coupled receptors. Mol Cell Neurosci 36:195–210.

Joseph EK, Levine JD (2010) Multiple PKCε-dependent mechanisms mediating mechanical hyperalgesia. Pain 150:17–21.

Kayser V, Elfassi IE, Aubel B, Melfort M, Julius D, Gingrich JA, Hamon M, Bourgoin S (2007) Mechanical, thermal and formalin-induced nocicption is differentially altered in 5-HT_{1A}−/−, 5-HT_{1B}−/−, 5-HT_{2A}−/−, 5-HT_{3A}−/−, 5-HTT−/− knock-out male mice. Pain 130:235–248.

Kessler W, Kirchhoff C, Reeh PW, Handwerker HO (1992) Excitation of cutaneous afferent nerve endings in vitro by a combination of inflammatory mediators and conditioning effect of substance P. Exp Brain Res 91:467–476.

Knight AR, Misra A, Quirk K, Benwell K, Revell D, Kennett G, Bickerdike M (2004) Pharmacological characterisation of the agonist radioligand binding site of 5-HT_{2A}, 5-HT_{2B} and 5-HT_{2C} receptors. Naunyn Schmiedebergs Arch Pharmacol 370:114–123.

Kress M, Reeh PW (1996) Chemical excitation and sensitization in nociceptors. In: Neurobiology of nociceptors (Cervero F, Belmonte C, eds), pp 258–297. New York: Oxford UP.

Millan MJ (1994) Serotonin and pain: evidence that activation of 5-HT_{1A} receptors does not elicit antinociception against noxious thermal, mechanical and chemical stimuli in mice. Pain 58:45–61.

Nicholson R, Small J, Dixon AK, Spanswick D, Lee K (2003) Serotonin receptor mRNA expression in rat dorsal root ganglion neurons. Neurosci Lett 337:119–122.

Parada CA, Tambeli CH, Cunha FQ, Ferreira SH (2001) The major role of peripheral release of histamine and 5-hydroxytryptamine in formalin-induced nociception. Pain 102:937–944.

Reeh PW, Steen KH (1996) Tissue acidosis in nociception and pain. Prog Brain Res 113:143–151.

Schmelz M, Schmidt R, Weidner C, Hilliges M, Torebjork HE, Handwerker HO (2003) Chemical response pattern of different classes of C-nociceptors to pruritogens and algogens. J Neurophysiol 89:2441–2448.

Sommer C (2004) Serotonin in pain and analgesia. In: Molecular neurobiology, Vol 30 (Bazan NG, Mallet J, eds), pp 117–125. Totowa, NJ: Humana.

Sufka KJ, Schomburg FM, Giordano J (1992) Receptor mediation of 5-HT-induced inflammation and nociception in rats. Pharmacol Biochem Behav 41:53–56.

Taiwo YO, Levine JD (1992) Serotonin is a directly-acting hyperalgesia agent in the rat. Neuroscience 48:485–490.

Tokunaga A, Saika M, Senba E (1998) 5-HT_{2A} receptor subtype is involved in the thermal hyperalgesic mechanism of serotonin in the periphery. Pain 76:349–355.

Wu S, Zhu M, Wang W, Wang Y, Li Y, Yew DT (2001) Changes of the expression of 5HT receptor subtype mRNAs in rat dorsal root ganglion by complete Freund's adjuvant-induced inflammation. Neurosci Lett 307:183–186.

Zeitz KP, Guy N, Malmberg AB, Dirajlal S, Martin WJ, Sun L, Bonhaus DW, Stucky CL, Julius D, Basbaum AI (2002) The 5-HT_3 subtype of serotonin receptor contributes to nociceptive processing via a novel subset of myelinated and unmyelinated nociceptors. J Neurosci 22:1010–1019.